

The LHCb VELO detector: design, operation and first results

Alice Biolchini on behalf of the LHCb VELO group^{a,*}

^a*Nikhef and Vrije Universiteit*

Science Park 105, 1098 XG Amsterdam, Netherlands,

E-mail: alice.biolchini@cern.ch

The LHCb detector is a single-arm spectrometer with a pseudorapidity range of $1.80 < \eta < 4.91$. The detector includes a high-precision tracking system consisting of a VERtEx LOcator detector (VELO) surrounding the interaction region and two more systems of trackers, placed upstream and downstream of the dipole magnet. LHCb underwent a major upgrade during the Long Shutdown 2 from 2019 to 2021. In order to increase the operational luminosity from $4 \times 10^{32} \text{ cm}^{-2} \text{ s}^{-1}$ to $20 \times 10^{32} \text{ cm}^{-2} \text{ s}^{-1}$ and to remove the hardware level trigger to readout at full rate (40 MHz). This article focuses on the design of the upgraded VELO and on few paramount commissioning steps such as equalisation procedure, time alignment and IV scans to assess radiation damage. Furthermore, it will cover one notable achievement: the closure of the VELO at the end of 2022 which led to the first mass peaks reconstruction (*e.g.* $D^0 \rightarrow K\pi$ peak). Finally, the RF-box incident happened in January 2023 will be discussed as well.

*The European Physical Society Conference on High Energy Physics (EPS-HEP2023)
21-25 August 2023
Hamburg, Germany*

*Speaker

1. VELO Upgrade design

The LHCb detector[1], a single-arm spectrometer with a pseudorapidity range from 1.80 to 4.91, plays a crucial role in studying particle physics phenomena. To enhance its capabilities and cope with increased luminosity and data rates, LHCb underwent a significant upgrade during the Long Shutdown 2 (2019-2021). Among the other upgraded sub-detectors, the VELO, a silicon vertex detector which surrounds the interaction region, is vital for triggering and reconstructing displaced vertices, as well it plays a significant role in tracking. The VELO[2] underwent significant improvements, which included replacing microstrips with pixels, upgrading electronics, and implementing a new cooling system. The upgraded VELO consists of two retractable halves, each of which houses an array of 26 L-shaped silicon pixel detector modules. The two halves are enclosed in boxes made of cast aluminium alloy, AlMg4.5Mn0.7 EN-AW5083, called RF-boxes. They avoid radio frequency pick up from the beam and provide continuity to the beam impedance. Furthermore, it separates the machine vacuum from the secondary vacuum in which the modules are located. All of this is housed inside a vacuum tank, as shown in Figure 1.

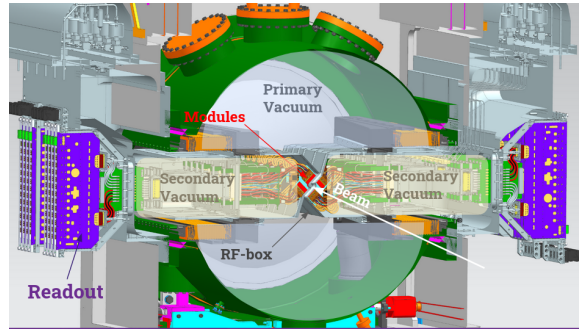


Figure 1: Scheme of the vacuum tank that hosts the modules of the VELO detector. The RF-boxes separate the modules from the primary beam vacuum.

1.1 Modules

The building blocks of the VELO are the modules shown in Figure 2. Each module is equipped with an highly thermally efficient cooling solution of evaporative CO₂ circulating in microchannels embedded in a silicon cooler, the microchannel substrate[3]. Each module has twelve VeloPix ASICs made by 256 × 256 square pixels (55 μm pitch), resulting in a sensitive area of 14.08 × 14.08 mm² per VeloPix ASIC. Three VeloPix ASICs are bump-bonded to a 200 μm thick silicon sensor to form a tile. Pairs of tiles are glued in a "L" shape onto either side of the microchannel cooler to ensure full coverage of the inner region.

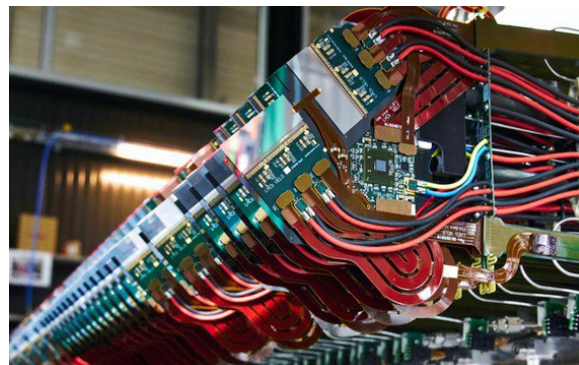


Figure 2: Picture of one half of the VELO, where the front hybrid of the array of the modules is visible. [CERN-PHOTO-202202-032](#)

2. Commissioning

A significant milestone was achieved during the initial months of Run 3 in 2022 with the commissioning of the upgraded VELO. This commissioning process involves several important steps, including equalising pixel responses, time alignment, and IV scans to evaluate radiation damage. These procedures are essential to ensure the proper functioning of the detector, which resulted in the first successful closure of the VELO to its intended position.

2.1 Equalisation

Equalisation refers to equalise the per-pixel response with respect to the same given input. A noise threshold is set for each ASIC, and it remains constant for all pixels, this is called global threshold (Th_{global}). However, by using the 4-bit fine-tuning offset parameter (trim) that each pixel has, it is possible to set a local threshold (Th_{local}) as follows:

$$Th_{local} = trim + Th_{global}. \quad (1)$$

The process begins by conducting threshold scans for the minimum and maximum values of the trim (0 and 15) for each pixel[4]. The decision to do this is based on the fact that it will offer the lowest and highest threshold that can be set per pixel. From each scan, a threshold is determined based on the noise rate. This process is repeated for all the 256x256 pixels of the ASIC. The sketch in Figure 3 illustrates the result of the threshold scans by plotting the noise rate calculated for all the pixels of an ASIC for the trim 0 (blue) and trim 15 (red) scans. To find the optimal trim value for each pixel, a target threshold is set at half the distance between the means of the two distributions. From the target threshold, a trim value per pixel is recomputed. This procedure establishes operational local thresholds per pixel. The final step of the equalisation is to set a global threshold. In order to do that, a threshold scan with the new trim values will be taken. Ideally, such ‘‘control’’ scan will produce a δ function around the target threshold. In practice, this will be a distribution peaking on the target threshold value, due to the trim resolution. The global threshold will be chosen per ASIC, taking into consideration that all the pixels with ‘‘control’’ scan above threshold will be masked and that a low threshold is more likely to leave noisy pixels. In order to test the results of the equalisation procedure, a noise run is used. No noisy pixels are expected to be seen from a noise run taken after equalisation. This is paramount in order to proceed with another important commissioning test: the time alignment.

To find the optimal trim value for each pixel, a target threshold is set at half the distance between the means of the two distributions. From the target threshold, a trim value per pixel is recomputed. This procedure establishes operational local thresholds per pixel. The final step of the equalisation is to set a global threshold. In order to do that, a threshold scan with the new trim values will be taken. Ideally, such ‘‘control’’ scan will produce a δ function around the target threshold. In practice, this will be a distribution peaking on the target threshold value, due to the trim resolution. The global threshold will be chosen per ASIC, taking into consideration that all the pixels with ‘‘control’’ scan above threshold will be masked and that a low threshold is more likely to leave noisy pixels. In order to test the results of the equalisation procedure, a noise run is used. No noisy pixels are expected to be seen from a noise run taken after equalisation. This is paramount in order to proceed with another important commissioning test: the time alignment.

2.2 Time Alignment

As a result of equalisation, a global threshold per ASIC has been calculated. Once the thresholds are set, it is possible to verify the time alignment of the detector. The goal of the time alignment

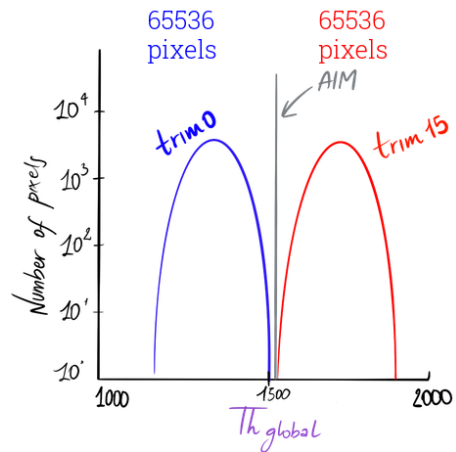


Figure 3: Sketch of the distributions of the threshold computed from the threshold scan performed per pixel. The trim values are set to 0 and 15, for the blue and red distributions, respectively.

procedure is to ensure that all ASICs respond synchronous to particle tracks produced from primary interactions. Specifically, this means ensuring that the recorded hits are assigned to the correct “bunch crossing” (bxID) from which they come from, and will not be assigned to earlier or later collisions. The bxIDs, each one of 25 ns, determine the LHC clock. Firstly, a coarse alignment in units of one bxID is performed. This is achieved by using an isolated bunch: comparing the VELO count when the signal is detected, to the known LHC clock count and adjusting the delay accordingly.

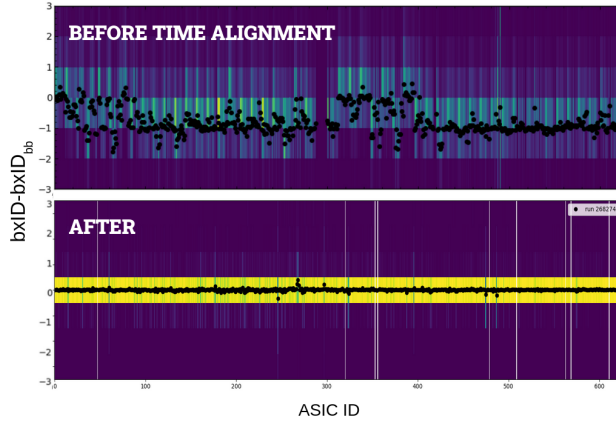


Figure 4: Difference between the VELO bunch cross ID (bxID) and the LHC bunch cross ID ($bxID_{bb}$), before and after the time alignment.

2.3 VELO closing procedure

A preliminary version of equalisation and time alignment enabled the reconstruction of tracks, allowing for a real-time vertex reconstruction. Thanks to which was possible to monitor the position of the beam, ensuring the safe positioning of the VELO around the interaction region. For the first closure of the VELO it was important to verify that the position and shape of the RF-boxes would leave a safe aperture for the beams to pass through. This verification was conducted through VELO tomography, which utilises the online vertex reconstruction with a minimum of 3 tracks. By reconstructing the interaction vertices of the particles with the material, it becomes possible to scan the RF-boxes position with respect to the interaction point. With the help of the online reconstruction of the beam position and the tomography technique, the VELO was successfully closed to its nominal position in November 2022.

The Figure 5 shows the projection on the xy plane of the interaction vertices integrating over the

Secondly, it is important to ensure that both low and high amplitude signals fall within the same LHC clock count. The delay caused by this effect is shorter than one bxID, meaning the shift can be of ± 1 bxID. The phases of the electronics are adjusted to regulate the delay of the VELO clock, in order to correct for this effect. The plot in Figure 4 illustrates the most recent time alignment. The vertical scale of the plot shows of how many bxIDs the VELO clock is off time with respect the LHC clock. The plot in the bottom shows that all the modules of the VELO are within ± 1 bxID with the LHC clock. Therefore, it confirms that time alignment procedure is in place.

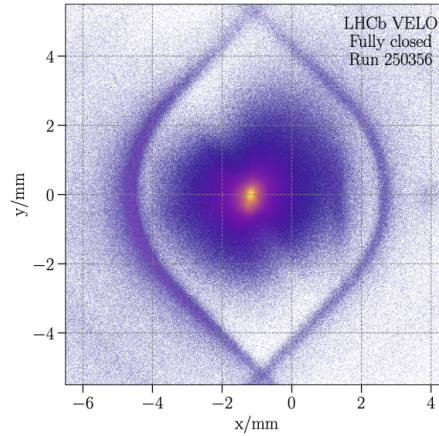


Figure 5: 2D histogram, showing the x and y positions of reconstructed vertices, with the VELO in the fully closed position. 215M vertices are plotted, from Run 250356.

z axis, when the VELO is in the fully closed position. The vertices shown in the plot are reconstructed independently by both VELO halves. The beam-spot is visible in the centre, positioned at -1 mm, due to an offset of the beam with respect VELO axis. The diffuse region around the beam spot corresponds to vertices from secondary decays. The inner edges of the RF-boxes are clearly seen, showing that the VELO halves are well centred around the beam. Being able to monitor the position of the modules and the RF-boxes almost in real time, it is extremely important. Since the VELO comes very close to the beam by design, deviations from expectation could both cause an unexpected beam dump and possible damage to the VELO itself.

2.4 IV Scans

The irradiation profile of the VELO strongly depends on the distance from the interaction point. As a consequence, modules that are closer to the interaction region ($z = 0$) are expected to accumulate more radiation damage. The result is an increase of the leakage current, among others effects[4]. Therefore, the IV (current vs voltage) scans are a fundamental tool in order to monitor this effect, and the evolution of the radiation damage with fluence. The linear relation that stands between fluence (Φ) and leakage current (ΔI) allows the computation of the current related damage rate (α) as follows:

$$\Delta I/vol = \alpha\Phi \quad (2)$$

where vol is the silicon volume[5]. The studies performed at end of 2022 show α values relatives to different modules along the VELO, to be consistent with each other, see results in Table 1. This suggests that the increase of the leakage current after data taking 2022 is compatible with scaling linearly with fluence and uniformly across the whole detector. No anomalous increase in current is observed.

	Module 15	Module 36	Module 44
z [mm]	0.00	262.50	587.50
α [$nA \times 10^{-12} cm^2 / MeV n_{eq}$]	14.45 ± 0.03	14.65 ± 0.04	13.2 ± 0.74

Table 1: The z -positions are given with respect to the nominal interaction point[6]. Values of the slope (α) from the I vs Φ fits for the reported modules[7].

3. RF-box incident

On January 10th 2023 there was a loss of control in the LHC vacuum safety system. A differential pressure of 200 mbar built up between primary and secondary volumes, whereas the boxes are designed to withstand only 10 mbar. After the incident, it was confirmed with leakage current measurements and by checking the response of the ASICs that the VELO modules were not damaged. However, RF-boxes have suffered plastic deformation up to 14 mm and have to be replaced. As the VELO was fully efficient for tracking, it was possible to measure the shape of the mechanics by reconstructing hadronic vertices in the material (tomography). This enabled to *see* the damage to the RF-boxes and define the limit of the VELO movement. Due to the incident, it was not possible to fully close the VELO in 2023, as had been done in 2022. The two halves were

kept 49 mm apart¹. The RF-boxes will be replaced during the 2023 year end technical stop, and be ready for data taking in 2024 when the LHC restart.

4. First results and conclusions

To conclude, in July 2022 the LHC Run3 started, and the first months were dedicated to the commissioning of the detector. In November 2022, the VELO has been fully closed. This has been done thanks to a preliminary version of equalisation, time and space alignment which allowed to perform online vertex reconstruction. The information from the VELO together with the other detectors allowed to successfully reconstruct the firsts mass peaks, such as the $D^0 \rightarrow K\pi$ mass peak[8]. In January 2023, a loss of control in the LHC vacuum safety system led to a plastic deformation of the RF-boxes which requires them to be replaced. The modules of the VELO were unharmed. However, the physics program for the year 2023 have been significantly affected because it was not possible to close the VELO. While, the commissioning can proceed as planned. This article covers a very small fraction of all the work that has been carried out in order to commission the detector. Needless to say, this is the result of the hard-work of several people.

References

- [1] A. A. Alves, Jr. *et al.* [LHCb], “The LHCb Detector at the LHC”, [doi:10.1088/1748-0221/3/08/S08005](https://doi.org/10.1088/1748-0221/3/08/S08005)
- [2] I. Bediaga [LHCb], “LHCb VELO Upgrade Technical Design Report”, [CERN-LHCC-2013-021](https://arxiv.org/abs/2013.021).
- [3] P. Collins *et al.* [LHCb], “Microchannel Cooling for the LHCb VELO Upgrade I”, [arXiv:2112.12763](https://arxiv.org/abs/2112.12763).
- [4] P. Svihra, Manchester U., “Developing a Silicon Pixel Detector for the Next Generation LHCb Experiment”, [CERN-THESIS-2021-309](https://arxiv.org/abs/2021.309)
- [5] M. Moll, “Radiation damage in silicon particle detectors: Microscopic defects and macroscopic properties”, [DESY-THESIS-1999-040](https://arxiv.org/abs/1999.040).
- [6] V. Coco *et al.* [LHCb Velo], “Velo Upgrade Module Nomenclature”, [LHCb-PUB-2019-008](https://arxiv.org/abs/2019.008).
- [7] G. Zunica, “Searches for CP violation in $D^0 \rightarrow K_S^0 K\pi$ decays with the Energy test method, module assembly and commissioning for the LHCb VELO Upgrade”, Manchester U., [CERN-THESIS-2023-144](https://arxiv.org/abs/2023.144)
- [8] LHCb Collaboration, “Mass plots with early Run 3 data”, [LHCb-FIGURE-2023-002](https://arxiv.org/abs/2023.002)

¹Gap between the two halves, which is the sum of the positions of the two sides of the VELO.